J. Fluid Mech. (1966), *vol.* 25, *part* 3, *pp.* 557–576
Printed in Great Britain

Steady three-dimensional vortex flow

By ROBERT GRANGER
Engineering Department, U.S. Naval Academy, Annapolis, Maryland

(Received 3 September 1965)

A theory is developed for an incompressible fluid in a steady three-dimensional rotational flow. Solutions are obtained subject to the restriction of small perturbations and are determinant provided that the vorticity distribution along the axis of rotation is known. Effects of viscosity are included. Closed-form expressions for the zeroth-order circulation and stream function and first-order circulation are given, with other higher-order expressions requiring high-speed computers. Experimental results of radial variation of axial velocity in the core show a distribution more elaborate than Gaussian.

1. Introduction

In recent years a number of writers have formulated the Navier–Stokes equations for steady axisymmetric flows. A brief review of the subject up to 1962 has been given by Lewellen (1962). Rott (1958) considers the case of a potential flow field where the radial velocity varies directly with the radius, and the axial velocity increases linearly along the axis of symmetry. The results show that while the vortex tends to decay, the flow carries new circulation from infinity towards the axis of symmetry.

Donaldson & Sullivan (1960) extend Rott's solution by considering a radial distribution of both radial and tangential velocity, such that the axial gradient of the radial distribution of pressure does not exist. This is unrealistic in many problems of rotational flow.

The results of Long (1961) are applicable for rotational flows near the region of a sink, and are useful for small values of circulation.

In the present paper, the writer adopts a procedure which is akin to that employed by Lewellen (1962), in his work on three-dimensional vortex motion. In § 2 the exact differential equations of motion are developed in terms of the circulation and the stream function for steady axisymmetric flow. In § 3, the circulation and stream function are expressed in a power-series expansion of the local radial Reynolds number. The differential equation for the zeroth-order circulation becomes the Tricomi equation, the solution of which can be found by use of the Maclaurin series. The zeroth-order circulation is shown to be dependent upon knowledge of the behaviour of the vorticity along the axis of rotation.

In § 4, the writer examines a few examples of rotational flow, each based upon a specific distribution of vorticity along the axis of rotation. In § 5, closed form expressions for the axial and radial velocities are derived. In § 6, the first-order

circulation is derived, followed by a discussion of elementary inviscid and viscid vortex flows. An exploratory experiment is presented in § 7 describing the salient features of the structure of a steady vortex sink.

2. Equations of motion

The Navier–Stokes equations for axisymmetric steady flow of an incompressible fluid medium expressed in cylindrical co-ordinates are

$$u\frac{\partial u}{\partial r}+w\frac{\partial u}{\partial z}-\frac{v^2}{r}=-\frac{1}{\rho}\frac{\partial p}{\partial r}+\nu\left[\frac{\partial^2 u}{\partial r^2}+\frac{1}{r}\frac{\partial u}{\partial r}-\frac{u}{r^2}+\frac{\partial^2 u}{\partial z^2}\right], \tag{1}$$

$$u\frac{\partial v}{\partial r}+w\frac{\partial v}{\partial z}+\frac{uv}{r}=\nu\left[\frac{\partial^2 v}{\partial r^2}+\frac{1}{r}\frac{\partial v}{\partial r}-\frac{v}{r^2}+\frac{\partial^2 v}{\partial z^2}\right], \tag{2}$$

$$u\frac{\partial w}{\partial r}+w\frac{\partial w}{\partial z}=-\frac{1}{\rho}\frac{\partial p}{\partial z}+\nu\left[\frac{\partial^2 w}{\partial r^2}+\frac{1}{r}\frac{\partial w}{\partial r}+\frac{\partial^2 w}{\partial z^2}\right]. \tag{3}$$

The continuity equation is

$$\frac{\partial u}{\partial r}+\frac{u}{r}+\frac{\partial w}{\partial z}=0. \tag{4}$$

The axisymmetric stream function ψ is introduced in order to reduce the number of dependent variables

$$u=\frac{1}{r}\frac{\partial \psi}{\partial z}, \tag{5}$$

$$w=-\frac{1}{r}\frac{\partial \psi}{\partial r}. \tag{6}$$

It is convenient to introduce the circulation Γ and relate it to the tangential velocity v through

$$\Gamma=rv. \tag{7}$$

Substituting equations (5) to (7) into equation (2) yields

$$\frac{1}{r}\frac{\partial \psi}{\partial z}\frac{\partial \Gamma}{\partial r}-\frac{1}{r}\frac{\partial \psi}{\partial r}\frac{\partial \Gamma}{\partial z}=\nu\left[\frac{\partial^2 \Gamma}{\partial r^2}-\frac{1}{r}\frac{\partial \Gamma}{\partial r}+\frac{\partial^2 \Gamma}{\partial z^2}\right]. \tag{8}$$

Eliminating the pressure gradients in equations (1) and (3) results in

$$\begin{aligned} r^2\left(2\nu+\frac{\partial \psi}{\partial z}\right)\left(\frac{\partial^3 \psi}{\partial r^3}+\frac{\partial^3 \psi}{\partial r\,\partial z^2}\right)-3r\frac{\partial^2 \psi}{\partial r^2}\left(\nu+\frac{\partial \psi}{\partial z}\right) \\ -2r\Gamma\frac{\partial \Gamma}{\partial z}+\left(3\frac{\partial \psi}{\partial z}+r\frac{\partial^2 \psi}{\partial r\,\partial z}-r^2\frac{\partial^3 \psi}{\partial r^2\,\partial z}-r^2\frac{\partial^3 \psi}{\partial z^3}+3\nu\right)\frac{\partial \psi}{\partial r} \\ -2r\frac{\partial \psi}{\partial z}\frac{\partial^2 \psi}{\partial z^2}-r^3\left(\frac{\partial^4 \psi}{\partial r^4}+2\nu\frac{\partial^4 \psi}{\partial r^2\,\partial z^2}+\nu\frac{\partial^4 \psi}{\partial z^4}\right)=0. \end{aligned} \tag{9}$$

Consider the following dimensionless parameters:

$$\eta\equiv(r/r_0)^2, \quad \xi\equiv z/l, \tag{10), (11}$$

$$\bar{\Gamma}\equiv\Gamma/\Gamma_\infty, \quad \bar{\psi}\equiv\psi/Ql, \tag{12), (13}$$

where r_0 and l are characteristic lengths in the radial and axial direction, respectively, and are constant. The potential field circulation $2\pi\Gamma_\infty$, and the radial

volume rate of flow per unit length $2\pi Q$ are both constant. Equations (8) and (9) are then expressed as

$$\frac{\partial\overline{\psi}}{\partial\xi}\frac{\partial\overline{\Gamma}}{\partial\eta}-\frac{\partial\overline{\psi}}{\partial\eta}\frac{\partial\overline{\Gamma}}{\partial\xi}=\frac{1}{N}\left(2\eta\frac{\partial^2\overline{\Gamma}}{\partial\eta^2}+\frac{\alpha}{2}\frac{\partial^2\overline{\Gamma}}{\partial\xi^2}\right), \tag{14}$$

$$\overline{\Gamma}\frac{\partial\overline{\Gamma}}{\partial\xi}=\epsilon\left\{4\eta^2\left[\frac{\partial\overline{\psi}}{\partial\xi}\frac{\partial^3\overline{\psi}}{\partial\eta^3}-\frac{\partial\overline{\psi}}{\partial\eta}\frac{\partial^3\overline{\psi}}{\partial\xi\,\partial\eta^2}-\frac{2}{N}\left(2\frac{\partial^3\overline{\psi}}{\partial\eta^3}+\eta\frac{\partial^4\overline{\psi}}{\partial\eta^4}\right)\right]\right.$$

$$\left.+\alpha\left[\eta\frac{\partial\overline{\psi}}{\partial\xi}\frac{\partial^3\overline{\psi}}{\partial\eta\,\partial\xi^2}-\frac{\partial\overline{\psi}}{\partial\xi}\frac{\partial^2\overline{\psi}}{\partial\xi^2}-\eta\frac{\partial\overline{\psi}}{\partial\eta}\frac{\partial^3\overline{\psi}}{\partial\xi^3}-\frac{1}{N}\left(4\eta^2\frac{\partial^4\overline{\psi}}{\partial\eta^2\,\partial\xi^2}+\frac{\alpha}{2}\eta\frac{\partial^4\overline{\psi}}{\partial\xi^4}\right)\right]\right\}, \tag{15}$$

where the local radial Reynolds number N is based upon the constant radial area rate of flow

$$N\equiv Q/\nu, \tag{16}$$

and where the Rossby number ϵ is defined as

$$\epsilon\equiv Ql/(\Gamma_\infty r_0), \tag{17}$$

and α is the geometric ratio

$$\alpha\equiv(r_0/l)^2. \tag{18}$$

The solutions of equations (14) and (15) are formidable since $\overline{\Gamma}$ and $\overline{\psi}$ are coupled. Therefore one must seek a means of uncoupling them.

3. The circulation

Lewellen assumed an asymptotic series in powers of Rossby number, but this assumption imposes limitations on the axial extent of the motion as well as on the magnitude of the radial velocity. The expansion of the circulation and stream function in powers of radial Reynolds number requires only that the radial velocity be small compared to the axial and tangential velocities. For instance, it was found experimentally that the radial velocity reached a maximum near the viscous core region of a vortex such that a maximum Reynolds number of $N = 0{\cdot}7$ was obtained based upon a maximum value of circulation,

$$\Gamma_\infty = 16\,\text{in.}^2/\text{sec}.$$

The variables are expanded in a power series of N

$$\overline{\Gamma}(\xi,\eta)=\overline{\Gamma}_0(\xi,\eta)+\overline{\Gamma}_1(\xi,\eta)\,N+\overline{\Gamma}_2(\xi,\eta)\,N^2+\ldots, \tag{19}$$

$$\overline{\psi}(\xi,\eta)=\overline{\psi}_0(\xi,\eta)+\overline{\psi}_1(\xi,\eta)\,N+\overline{\psi}_2(\xi,\eta)\,N^2+\ldots. \tag{20}$$

Substituting equations (19) and (20) into equations (14) and (15) and equating coefficients of powers of N yields a set of equations. The coefficients of N^0 are

$$2\eta\frac{\partial^2\overline{\Gamma}_0}{\partial\eta^2}+\frac{\alpha}{2}\frac{\partial^2\overline{\Gamma}_0}{\partial\xi^2}=0 \tag{21}$$

from equation (14) and

$$8\eta^2\left(2\frac{\partial^3\overline{\psi}_0}{\partial\eta^3}+\eta\frac{\partial^4\overline{\psi}_0}{\partial\eta^4}\right)+\alpha\left(4\eta^2\frac{\partial^4\overline{\psi}_0}{\partial\eta^2\,\partial\xi^2}+\frac{\alpha}{2}\eta\frac{\partial^4\overline{\psi}_0}{\partial\xi^4}\right)=0 \tag{22}$$

from equation (15). The coefficients of N yield

$$2\eta\frac{\partial^2\overline{\Gamma}_1}{\partial\eta^2}+\frac{\alpha}{2}\frac{\partial^2\overline{\Gamma}_1}{\partial\xi^2}=\frac{\partial\overline{\psi}_0}{\partial\xi}\frac{\partial\overline{\Gamma}_0}{\partial\eta}-\frac{\partial\overline{\psi}_0}{\partial\eta}\frac{\partial\overline{\Gamma}_0}{\partial\xi}, \tag{23}$$

$$\begin{aligned}8\eta^2\left(2\frac{\partial^3\overline{\psi}_1}{\partial\eta^3}+\eta\frac{\partial^4\overline{\psi}_1}{\partial\eta^4}\right)+\alpha\left(4\eta^2\frac{\partial^4\overline{\psi}_1}{\partial\eta^2\partial\xi^2}+\frac{\alpha}{2}\eta\frac{\partial^4\overline{\psi}_1}{\partial\xi^4}\right)\\ =-\frac{1}{\epsilon}\overline{\Gamma}_0\frac{\partial\overline{\Gamma}_0}{\partial\xi}+4\eta^2\frac{\partial\overline{\psi}_0}{\partial\xi}\frac{\partial^3\overline{\psi}_0}{\partial\eta^3}-4\eta^2\frac{\partial\overline{\psi}_0}{\partial\eta}\frac{\partial^3\overline{\psi}_0}{\partial\eta^2\partial\xi}\\ -\alpha\left[\frac{\partial\overline{\psi}_0}{\partial\xi}\frac{\partial^2\overline{\psi}_0}{\partial\xi^2}-\eta\frac{\partial\overline{\psi}_0}{\partial\xi}\frac{\partial^3\overline{\psi}_0}{\partial\eta\partial\xi^2}+\eta\frac{\partial\overline{\psi}_0}{\partial\eta}\frac{\partial^3\overline{\psi}_0}{\partial\xi^3}\right].\end{aligned} \tag{24}$$

It is interesting to note that when $N = 0$, one has the potential solution such that the zeroth-order circulation represents the circulation of the entire flow. Classically, this is a circular Couette flow where the only finite velocity is the circular velocity composed of a superposition of a solid-body rotation and a potential vortex. It is shown in example A, § 4, that the present solution precisely accounts for this two-dimensional rotational flow.

The differential equation for the zeroth-order circulation is thus the Tricomi equation, with boundary conditions

$$\overline{\Gamma}_0(\xi,0)=0, \tag{25}$$

$$\partial\overline{\Gamma}_0(\xi,0)/\partial\eta=(\pi r_0^2/\Gamma_\infty)\gamma_0(\xi), \tag{26}$$

$$\overline{\Gamma}_0(\xi,\infty)=1, \tag{27}$$

$$\partial\overline{\Gamma}_0(\xi,\infty)/\partial\eta=0, \tag{28}$$

where $\gamma_0(\xi)$ is the vorticity on the centre line. The solution of equation (21) for the zeroth-order circulation is based upon the Maclaurin series with boundary conditions given by equations (25) and (26);

$$\overline{\Gamma}_0(\xi,\eta)=\overline{\Gamma}_0(\xi,0)+\eta\frac{\partial\overline{\Gamma}_0(\xi,0)}{\partial\eta}+\frac{\eta^2}{2!}\frac{\partial^2\overline{\Gamma}_0(\xi,0)}{\partial\eta^2}+\ldots. \tag{29}$$

The justification for using a power-series expansion about $\eta = 0$ stems from an examination of the general vorticity equation in a region not too far removed from the core of the vortex. The vorticity $\gamma(\xi,\eta)$ is continuous within a large area and on its boundary, whose centre is on the axis of symmetry of the function. Furthermore, the derivatives $\partial\gamma/\partial\xi$, $\partial\gamma/\partial\eta$ are likewise continuous and the second derivatives are finite and integrable. It is then possible to show that the vorticity, and subsequently the circulation, can be expanded in a power series of ascending power of η, ξ of a point relative to the axis of symmetry. Then the solution of the general vorticity equation becomes

$$\gamma(\xi,\eta)=\frac{1}{\pi}\int_0^\pi\gamma(z+ir\cos\phi)\,d\phi, \tag{30}$$

where a necessary requirement is that the solution reduces to $\gamma_0(\xi)$, when $\eta = 0$.

By successively differentiating equation (21) with respect to η and applying the boundary conditions of equations (25) and (26), one can obtain the various values of the coefficients in equation (29)

$$\frac{\partial^n \bar{\Gamma}_0(\xi,0)}{\partial \eta^n} = \frac{\pi r_0^2}{\Gamma_\infty}\left(-\frac{\alpha}{4}\right)^{n-1}\frac{1}{(n-1)!}\left(\frac{d}{d\xi}\right)^{2n-2}\gamma_0, \tag{31}$$

for $n = 1, 2, 3, \ldots$. Substituting equation (31) into equation (29) yields the expression for the zeroth-order circulation as a function of the vorticity distribution along the centre line

$$\bar{\Gamma}_0(\xi,\eta) = \frac{\pi r_0^2}{\Gamma_\infty}\left[\eta\gamma_0 - \frac{\alpha}{4}\frac{\eta^2}{2}\gamma_0'' + \frac{\alpha^2}{4.4.2!}\frac{\eta^3}{3!}\gamma_0^{\mathrm{iv}} - \frac{\alpha^3}{4.4.4.3!}\frac{\eta^4}{4!}\gamma_0^{\mathrm{vi}} + \ldots + \left(-\frac{\alpha}{4}\right)^{n-1}\frac{\eta^n}{n!}\frac{\gamma_0^{(2n-2)}}{(n-1)!} + \ldots\right]. \tag{32}$$

The stability of the solution is dependent upon the vorticity distribution $\gamma_0(\xi)$. Depending upon the type of vortex motion, one can derive an analytic expression for $\gamma_0(\xi)$ such that the circulation is definable throughout the entire flow régime. This will be illustrated in § 4.

4. Examples of vortex motion

Example A: the Rankine vortex

Consider the steady inviscid flow in a plane where the rotation is constant in the radial direction. This occurs solely within the core of a vortex (the core radius being defined as that value of radius when the free vortex surface is the forced vortex surface. See Appendix A). For this case

$$\gamma = \Gamma_\infty/(\pi r_0^2) \quad (0 \leqslant r \leqslant r_0) \tag{33}$$

and is illustrated in figure 1. Substituting equation (33) into equation (32) yields the circulation

$$\bar{\Gamma}_0 = r^2/r_0^2 \quad (0 \leqslant r \leqslant r_0), \tag{34}$$

also illustrated in figure 1.

One notes in figure 1, that for $\eta < 1$ the flow is solid-body rotation, whereas for $\eta > 1$ the flow is the potential vortex flow, and hence this motion is circular Couette flow.

Example B: three-dimensional vortices

(*a*) *Rott's vortex*

To derive the centre-line vorticity for the vortex motion of Rott (1958) one seeks a solution of the steady-flow vorticity equation

$$\nu\frac{\partial^2\gamma}{\partial r^2} + \left(\frac{\nu}{r} - u\right)\frac{\partial\gamma}{\partial r} + \nu\frac{\partial^2\gamma}{\partial z^2} = 0. \tag{35}$$

For the case of r very small

$$\left(\frac{\nu}{r} - u\right)\frac{\partial\gamma}{\partial r} \approx \frac{\nu}{r}\frac{\partial\gamma}{\partial r}. \tag{36}$$

The solution where the vorticity is of separable form is investigated first,

$$\gamma(r,z) = \gamma_0(z)R(r). \tag{37}$$

Substituting equations (37) and (36) into equation (35) and integrating yields

$$\gamma_0(\xi) = \{\Gamma_\infty/(\pi r_0^2)\}\exp[(2/\sqrt{\alpha})\xi]. \tag{38}$$

Consider a circulation

$$\bar{\Gamma}_0(\xi,\eta) = 1-\exp[-e^{-[(2/\sqrt{\alpha})\xi]}\eta]. \tag{39}$$

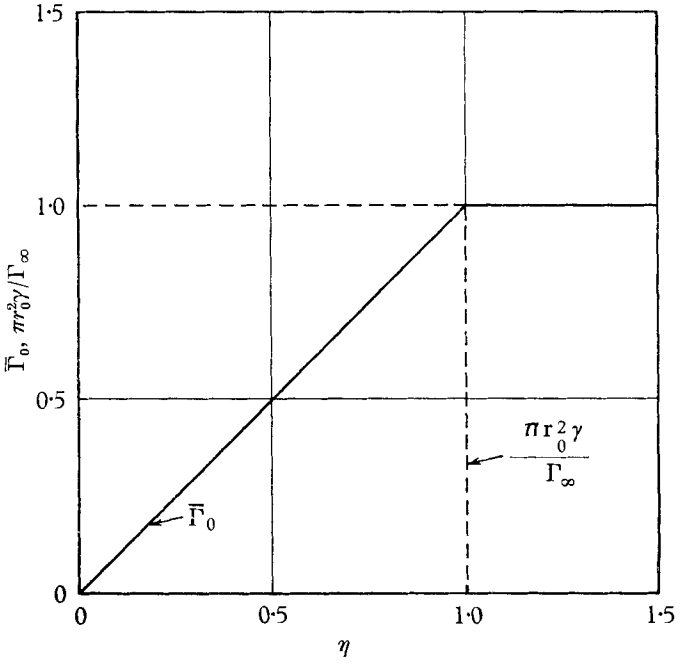

FIGURE 1. Radial distribution of vorticity and circulation for the Rankine vortex.

Equation (39) satisfies all the boundary conditions of equations (25)–(28), and yields the vorticity distribution described by equation (38). In addition, the vortex motion described by equation (39) reduces to Rott's vortex when surface conditions ($\xi = 0$) are imposed,

$$\bar{\Gamma}_0(0,\eta) = 1-e^{-\eta}. \tag{40}$$

However, substitution of equation (38) into equation (32) yields for $\xi = 0$

$$\bar{\Gamma}_0(0,\eta) = 1-\left[1-\eta+\frac{\eta^2}{2!}-\frac{1}{2!}\frac{\eta^3}{3!}+\ldots+\frac{(-1)^n}{(n-1)!}\frac{\eta^n}{n!}+\ldots\right], \tag{41}$$

or alternatively

$$\bar{\Gamma}_0(0,r) = \frac{r}{r_0}J_1\left(\frac{2r}{r_0}\right)H\left(\frac{2r}{r_0}\right). \tag{42}$$

The circulatory motion described by equation (42) has been derived by Burgers (1956) utilizing Lamb's equation. Burgers discusses the restrictions on η and the similarity of this type of rotational motion with those examined by several other investigators.

If one assumes the vorticity distribution

$$\gamma_0(\xi) = \frac{\Gamma_\infty}{\pi r_0^2} \tanh \frac{2}{\sqrt{\alpha}} \xi \tag{43}$$

and then sets

$$\xi = 0{\cdot}44\sqrt{\alpha}, \tag{44}$$

which is a statement of the condition very close to the surface (since α is usually a very small quantity), one can obtain equation (40) by substituting equation (43) into equation (32). Equation (43) is derived from equation (35) utilizing the near-surface condition of equation (44). Rott's vortex can thus be obtained by a judicious choice of vorticity distribution.

(*b*) *Alternative form of the three-dimensional vortex*

With r and z as independent variables, an obvious alternative solution for the vorticity is the infinite power series

$$\gamma(r,z) = \sum_{m,n} a_{m,n} z^m r^n. \tag{45}$$

By seeking an expression for the vorticity distribution solely along the centre line, the only coefficients that are of interest in equation (45) are those for $n = 0$. Substituting equations (45) and (36) into equation (35) and equating like powers of the variables yields

$$\left.\begin{aligned}
a_{1,0} &= 0,\\
a_{2,0} &= -\tfrac{4}{2}a_{0,2},\\
a_{3,0} &= -\tfrac{4}{6}a_{1,2} = 0,\\
a_{4,0} &= -\tfrac{4}{12}a_{2,2} = \tfrac{4}{12}\cdot\tfrac{16}{6}a_{0,4},\\
a_{5,0} &= -\tfrac{4}{20}a_{3,2} = \tfrac{4}{20}\cdot\tfrac{16}{6}a_{1,4} = 0,\\
a_{6,0} &= -\tfrac{4}{30}a_{4,2} = \tfrac{4}{30}\cdot\tfrac{16}{12}a_{2,4} = \tfrac{4}{30}\cdot\tfrac{16}{12}\cdot\tfrac{18}{1}a_{0,6},\\
&\vdots
\end{aligned}\right\} \tag{46}$$

Rott's solution at the surface can be satisfied by making

$$\left.\begin{aligned}
a_{0,2k+1} &= 0,\\
a_{0,2k} &= (-1)^k \frac{1}{k!}\left(\frac{1}{r_0}\right)^{2k} \quad (k = 0, 1, 2, \ldots).
\end{aligned}\right\} \tag{47}$$

Substituting equations (46) and (47) into equation (45) yields

$$\gamma_0(z) = \frac{\Gamma_\infty}{\pi r_0^2}\left[1 + 2\left(\frac{z}{r_0}\right)^2 + \frac{4}{3}\left(\frac{z}{r_0}\right)^4 + \frac{8}{15}\left(\frac{z}{r_0}\right)^6 + \ldots\right]. \tag{48}$$

Figure 2 shows that the vortex with $\gamma_0(z)$ given by equation (48) is stronger than the vortex given by equation (38).

Many other vortex motions can be analysed through knowledge of $\gamma_0(\xi)$. Consider a vortex that has a motion similar to an Oseen vortex of the form

$$\gamma(r,z) = f(z)\, e^{-f(z) r^2}. \tag{49}$$

Substituting equation (49) into equation (35) yields

$$(f'' - 4f^2)(1 - fr^2) + r^2 f'^2 (fr^2 - 2) = 0. \tag{50}$$

The vorticity at the centre line $\gamma_0(\xi)$ is thus

$$\gamma_0(z) = f(z), \tag{51}$$

such that equation (50) becomes

$$f'' - 4f^2 = 0. \tag{52}$$

The solution of equation (52) is

$$f = \wp(\sqrt{\tfrac{2}{3}}z), \tag{53}$$

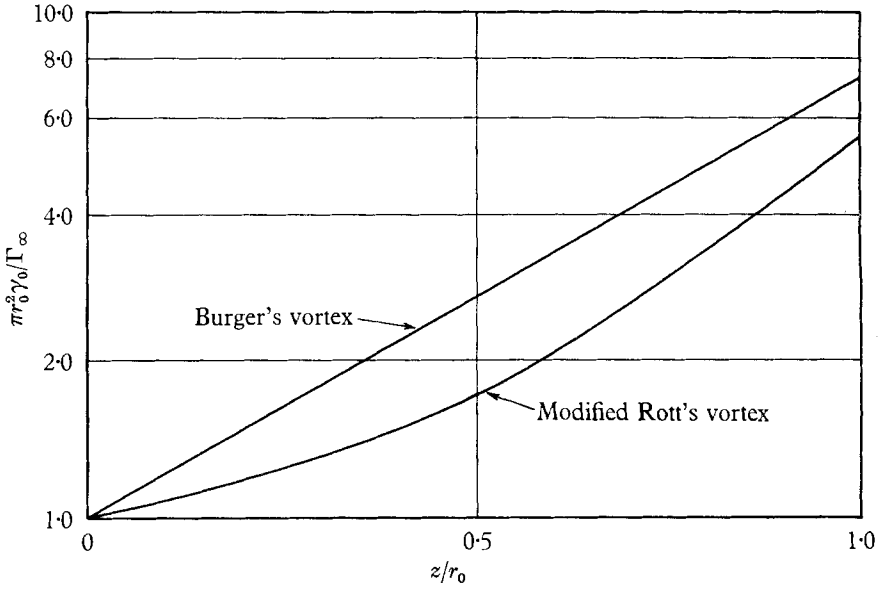

FIGURE 2. Axial distribution of centre-line vorticity for two similar vortices.

where $\wp$ is the elliptical function of the Weierstrass canonical form. With conditions of zero vorticity at the boundary, equation (53) becomes

$$f = 1{\cdot}5/z^2. \tag{54}$$

The zeroth-order circulation $\overline{\Gamma}_0(\xi, \eta)$ can be found by substituting equation (54) into equation (32) yielding

$$\overline{\Gamma}_0(\xi,\eta) = 1{\cdot}5\left[\chi - \frac{\alpha}{4}\frac{3!}{1!}\frac{\chi^2}{2!} + \frac{\alpha^2}{4.4}\frac{5!}{2!}\frac{\chi^3}{3!} - \ldots(-1)^{n-1}\left(\frac{\alpha}{4}\right)^{n-1}\frac{(2n-1)!}{(n-1)!}\frac{\chi^n}{n!} + \ldots\right], \tag{55}$$

where

$$\chi \equiv \eta/\xi^2. \tag{56}$$

5. The stream function

The differential equation for the zeroth-order stream function $\overline{\psi}_0$ is given by equation (22), with boundary conditions

$$\partial\psi(\xi,\infty)/\partial\eta = 0, \tag{57}$$

$$\partial\psi(\xi,0)/\partial\eta = \tfrac{1}{2}r_0^2 w_0(\xi), \tag{58}$$

$$\partial\psi(\xi,0)/\partial\xi = 0, \tag{59}$$

$$\partial\psi(\xi,\infty)/\partial\xi = 0, \tag{60}$$

where $w_0(\xi)$ is the axial velocity along the axis of symmetry. By use of the transformation

$$\chi \equiv \eta/\xi^2 \equiv x/\alpha, \tag{61}$$

and by defining

$$p \equiv d\overline{\psi}_0/d\chi, \tag{62}$$

equation (22) can be expressed as

$$\chi(\alpha\chi+1)^2\frac{d^3p}{d\chi^3}+(9\alpha^2\chi^2+3\alpha\chi+2)\frac{d^2p}{d\chi^2}+\frac{150}{8}\alpha^2\chi\frac{dp}{d\chi}+\frac{60}{8}\alpha^2p=0. \tag{63}$$

Because of repeated roots in the indicial equations, equation (63) is approximately satisfied by

$$\chi(\alpha\chi+1)^2\frac{d^2p}{d\chi^2}+(6\alpha^2\chi^2-\alpha\chi+1)\frac{dp}{d\chi}+(\tfrac{54}{8}\alpha^2\chi+\alpha)p=c. \tag{64}$$

Use is made of the method of Frobenius. Substituting the infinite power series

$$p=\sum_n a_n\chi^n \tag{65}$$

into equation (64), the coefficients of equation (65) are evaluated and found to be

$$a_n=-\alpha/n^2\{(n-2)(2n-3)a_{n-1}+\alpha[\tfrac{54}{8}+(n-2)(n+3)]a_{n-2}\}, \tag{66}$$

for $n=2,3,4,\ldots$, where a_1, a_0, c are evaluated from the boundary conditions of equations (57) and (58). Integration of equation (65) yields

$$\begin{aligned}\frac{\psi_0}{z^2w_0}=\;&0{\cdot}5x-0{\cdot}2817x^3+0{\cdot}0705x^4+0{\cdot}1836x^5\\&-0{\cdot}15x^6-0{\cdot}028x^7+0{\cdot}152x^8-0{\cdot}1455x^9\\&+0{\cdot}029x^{10}+0{\cdot}096x^{11}-0{\cdot}151x^{12}+0{\cdot}115x^{13}\\&-0{\cdot}02x^{14}-0{\cdot}0755x^{15}+\ldots.\end{aligned} \tag{67}$$

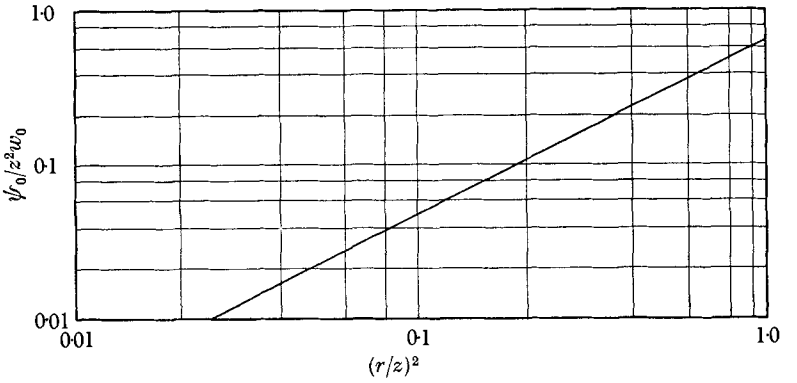

FIGURE 3. Zeroth-order stream function ψ_0.

It is seen from figure 3 that

$$\psi_0=0{\cdot}434r^2w_0 \tag{68}$$

is a good first approximation to equation (67). For instance, if the axial velocity along the centre line is a constant, then by equations (68) and (5), there can be no radial velocity. However, equation (68) states that there exists no radial

variation of the axial velocity and is therefore too restrictive for our analysis but does complement Rott's results.

It can be noted further from equation (68) that the stream tube radius is inversely proportional to the square root of the centre-line velocity. One suspects that such a conclusion would not exist in the forced flow field where viscosity effects are large. The higher-order circulation terms would have to be included for precise evaluation of the velocity field and will be discussed in § 6. In the region where $N \approx 0$, the results of the zeroth-order approximations are fair when compared with the experimental results shown in § 7.

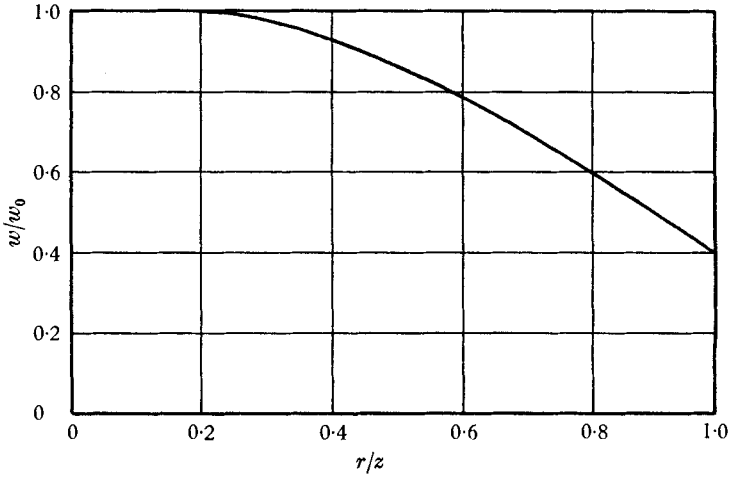

FIGURE 4. Axial velocity profile for vortex sink flow.

The axial and radial velocities are found by substituting equation (67) into equations (6) and (5) resulting in

$$w/w_0(\xi) = 1 - 1{\cdot}699x^2 + 0{\cdot}564x^3 + 1{\cdot}826x^4 - 1{\cdot}788x^5 + \ldots, \tag{69}$$

for the axial velocity and

$$u/w_0(\xi) = x^{\frac{1}{2}}[1{\cdot}1266 - 0{\cdot}423x - 1{\cdot}4688x^2 + 1{\cdot}49x^3 + \ldots] + \tfrac{1}{2}(\alpha\eta)^{\frac{1}{2}}\frac{w_0'}{w_0}[1 - 0{\cdot}5633x^2 + 0{\cdot}114x^3 + 0{\cdot}3672x^4 - \ldots], \tag{70}$$

for the radial velocity. Higher-degree terms can be obtained by use of the recursion formula of equation (56). The axial velocity is illustrated in figure 4.

6. First-order circulation

In § 3 the circulation of zeroth order, $\bar{\Gamma}_0(\xi, \eta)$, was developed and applied to flows that were principally potential, i.e. where the local radial Reynolds number is small or zero. The case where $N = 0$ requires that one of three conditions be satisfied: (i) application to very viscous fluids such that the rotational motion is solid-body rotation; (ii) application to rotational but inviscid fluids such that the radial volume rate per unit length, Q, is zero, or (iii) application to viscous

fluids where the radial diffusion of vorticity along the vortex axis is such that the axial flux remains constant along the axis. Many one-celled vortices where air is not sucked into the axis of rotation are such that, for negligibly small values of N, the zeroth-order circulation $\overline{\Gamma}_0$ and stream function $\overline{\psi}_0$ will suffice for calculating the steady-flow field. In this section, the effect of viscosity on the motion of vortex flows is discussed. To find the effect of viscosity, one would have to include higher-order terms $\overline{\Gamma}_1$, $\overline{\psi}_1$, $\overline{\Gamma}_2$, $\overline{\psi}_2$, etc.

The first-order circulation $\overline{\Gamma}_1(\xi, \eta)$ is found in the same manner as $\overline{\Gamma}_0(\xi, \eta)$. A Maclaurin expansion about the centre line yields

$$\overline{\Gamma}_1(\xi, \eta) = \overline{\Gamma}_1(\xi, 0) + \eta \frac{\partial \overline{\Gamma}_1}{\partial \eta}(\xi, 0) + \frac{\eta^2}{2!} \frac{\partial^2 \overline{\Gamma}_1}{\partial \eta^2}(\xi, 0) + \ldots, \tag{71}$$

with the boundary conditions

$$\overline{\Gamma}_1(\xi, 0) = 0, \quad \partial \overline{\Gamma}_1(\xi, 0)/\partial \eta = 0, \tag{72), (73}$$

where the vorticity at the centre line has previously been specified by equation (26). From equations (23) and (73), one obtains

$$\frac{\partial^2 \overline{\Gamma}_1(\xi, 0)}{\partial \eta^2} = \frac{1}{2}\left[\frac{\partial}{\partial \eta}\left(\frac{\partial \overline{\psi}_0}{\partial \xi}\frac{\partial \overline{\Gamma}_0}{\partial \eta} - \frac{\partial \overline{\psi}_0}{\partial \eta}\frac{\partial \overline{\Gamma}_0}{\partial \xi}\right)\right]_{\eta=0}. \tag{74}$$

Substituting equations (32) and (67) into equation (74) yields

$$\frac{\partial^2 \overline{\Gamma}_1(\xi, 0)}{\partial \eta^2} = \frac{\pi r_0^2 \alpha l}{4 \Gamma_\infty Q}(\gamma_0 w_0' - w_0 \gamma_0'). \tag{75}$$

In a similar manner, one obtains from equations (23) and (75)

$$\frac{\partial^3 \overline{\Gamma}_1(\xi, 0)}{\partial \eta^3} = \frac{\pi r_0^2 \alpha^2 l}{16 \Gamma_\infty Q}(w_0 \gamma_0''' - \gamma_0 w_0'''), \tag{76}$$

and from equations (23) and (76)

$$\frac{\partial^4 \overline{\Gamma}_1(\xi, 0)}{\partial \eta^4} = \frac{\pi r_0^2 \alpha^3 l}{192 \Gamma_\infty Q}(\gamma_0 w_0^{\mathrm{v}} - w_0 \gamma_0^{\mathrm{v}}), \tag{77}$$

such that the first-order circulation becomes

$$\overline{\Gamma}_1(\xi, \eta) = \frac{\pi r_0^2 l}{\Gamma_\infty Q}\left[\frac{\alpha}{4}(\gamma_0 w_0' - w_0 \gamma_0')\frac{\eta^2}{2!} - \left(\frac{\alpha}{4}\right)^2 (\gamma_0 w_0''' - w_0 \gamma_0''')\frac{\eta^3}{3!} + \left(\frac{\alpha}{4}\right)^3 \tfrac{1}{3}(\gamma_0 w_0^{\mathrm{v}} - w_0 \gamma_0^{\mathrm{v}})\frac{\eta^4}{4!} - \ldots\right]. \tag{78}$$

One notes that $\overline{\Gamma}_1(\xi, \eta) = 0$ for circular Couette flow, as should be the case. In addition, one notes from equation (78) that a necessary condition for potential flow is that the axial velocity at the centre line be similar to the vorticity distribution along the centre line, i.e.

$$\gamma_0(\xi)/w_0(\xi) = \text{const.}, \tag{79}$$

where the constant could have the values zero or infinity. For instance, consider those flow situations where the tangential velocity can vary only radially. It then follows from the definition of vorticity,

$$\gamma = \frac{v}{r} + \frac{\partial v}{\partial r}, \tag{80}$$

that vorticity can vary only in a radial direction. Introducing this restriction in equation (2) and integrating yields

$$\gamma(r) = A\, e^{1/\nu \int u\, dr}, \tag{81}$$

where A is an arbitrary constant of integration. Consider the following elementary examples:

Example C: Solid-body rotation

If the radial velocity u is zero everywhere in the flow field, the flow is said to rotate as a solid body at an angular velocity ω, such that, from equation (81),

$$\gamma = 2\omega. \tag{82}$$

In addition, the local radial Reynolds number N is also zero, from the definition by equation (16), which makes equation (79) applicable to solid-body rotation. From continuity, one finds that the centre-line axial velocity cannot vary in the axial direction, and usually is assumed zero.

Example D: Free vortex

A free vortex is characterized by two conditions:

(i) A linear radial distribution of radial velocity,

$$u = -ar, \tag{83}$$

which can result in a linear axial distribution of axial velocity

$$w = 2az \tag{84}$$

upon integration of the continuity equation.

(ii) Viscous effects are zero for the free vortex, such that from equations (83) and (84) one obtains zero vorticity everywhere in the flow field. Hence, the constant in equation (79) is zero for the case of a free vortex. One finds the tangential velocity

$$v = \Gamma_\infty/(2\pi r) \tag{85}$$

by integration of equation (80) and by using the definition of circulation Γ_∞. The solutions given by equations (83), (84) and (85) for the velocity field of a free vortex are thereby exact solutions of the Navier–Stokes equations.

Examples C and D set the upper and lower limits of a class of rotational flows where the tangential velocity varies only in a radial direction, and where $N = 0$.

For those flow situations where equation (79) is violated, i.e. where the ratio of this vorticity to axial velocity at the centre line is some function of ξ, an improved expression over the zeroth-order circulation is, from equation (19),

$$\overline{\Gamma}(\xi, \eta) \approx \overline{\Gamma}_0(\xi, \eta) + \overline{\Gamma}_1(\xi, \eta)\, N. \tag{86}$$

In those instances where $\alpha \ll 1$, one may consider solely the first terms in the $\overline{\Gamma}_1(\xi, \eta)$ expression given by equation (78), since viscous effects are important in flow fields where $r \leqslant r_c$, r_c being the core radius discussed in Appendix 1. Therefore, viscous effects can be studied for small values of N by comparing $\overline{\Gamma}_1 N$

with $\bar{\Gamma}_0$, where the first-order circulation given by equation (78) is approximated by

$$\bar{\Gamma}_1(\xi,\eta)N \approx \operatorname{sgn}\frac{\alpha l}{8\nu}\frac{\pi r_0^2}{\bar{\Gamma}_\infty}(\gamma_0 w_0' - w_0\gamma_0')\eta^2 \tag{87}$$

for $r \leqslant r_c$, where sgn is positive for radial outflow and negative for radial inflow.

For a negative value of radial velocity, i.e. $N < 0$, the fluid is moving radially toward the axis of symmetry and accelerating axially toward the sink. For flows of this type, the experiment as presented in § 7, was devised. The results shown in figure 7 show negative curvature for vorticity γ_0, and positive curvature for axial velocity w_0 such that the sgn of equation (87) is negative.

For a positive value of radial velocity, i.e. $N > 0$, the fluid is moving radially out of a cylindrical flow, and a vorticity distribution with positive curvature is permissible, such as the vorticity distribution given by equation (38). The sgn of $\bar{\Gamma}_1 N$ in equation (87) is negative.

There are some viscous flows that can be approximated with some degree of accuracy by the potential solution. For example, consider the limiting case of Burgers (1956), where $N = -\infty$. Such a case is not directly applicable to our perturbation technique owing to the infinite value of N. Burgers considers the velocity distributions of equations (83) and (84). The vorticity $\gamma(r)$ for such velocity profiles is, from equation (81),

$$\gamma(r) = \frac{a\Gamma_\infty}{2\pi\nu}e^{-ar^2/2\nu}. \tag{88}$$

The tangential velocity is found by substituting equation (88) into equation (80) and integrating. The result of the integration is

$$v = \frac{\Gamma_\infty}{2\pi r}(1 - e^{-ar^2/2\nu}). \tag{89}$$

However, the rotational flow described by equation (89) is precisely the rotational flow given by equation (40) if one sets

$$r_0^2 = 2\nu/a. \tag{90}$$

Thus viscous flows of certain types can be treated by examination of the zeroth-order circulation $\bar{\Gamma}_0$. The solution is dependent upon judicious choice of the expression for the vorticity distribution along the centre line.

7. Exploratory experiment on the structure of a steady vortex sink

7.1. *Experimental apparatus*

The principal experimental investigation was conducted with water as a working fluid in a cylindrical vortex tank, illustrated schematically in figure 5.

The tank was 4 ft. high and 23 in. in diameter. It could be filled with water to within a few inches of its rim. There were two concentric cylindrical walls both made of clear plastic sheets, an outer wall firmly mounted in the horizontal tank table so as to create a water-tight container and the inner cylindrical wall inserted into the former so as to form a narrow annular space of $\frac{1}{2}$ in. radial width. The water circulating through the tank was admitted to this annular space

through 8 vertical tubes equally spaced about the perimeter, the walls of which were perforated by equally spaced small holes so as to distribute the entering water uniformly in a vertical direction. Numerous holes were punched with uniform spacing in the inner cylindrical wall, each hole provided with a hood to direct the jets of water tangentially along the inner cylindrical surface. In this way, a circulation was imparted to the body of water filling the central space of

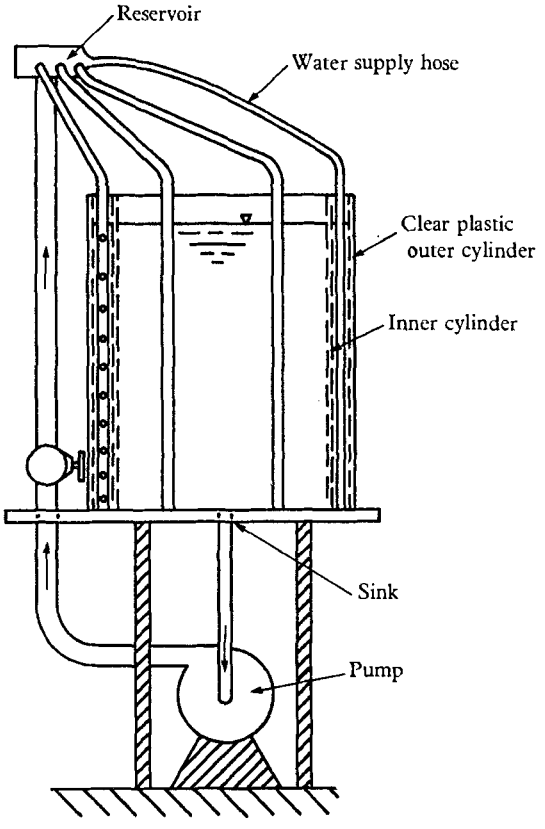

FIGURE 5. Schematic of vortex generator.

the tank. The circulated water was removed through a central hole located on the bottom surface of the tank. Thence the water passed through a remote-controlled shutoff valve to a centrifugal pump placed into the external closed circuit, then through a throttle valve, and finally to a header back into the admission tubes of the tank.

7.2. *Measurements of the undisturbed flow of the vortex sink*

Steady laminar flow was achieved in the field of the vortex sink which was produced in the vortex tank described previously. By systematic survey measurements it was found that the turbulence which was created in the mixing zone of the tangential influx jets died off within 4 in. of the inner cylindrical wall of the tank. Similarly, the influence of the boundary layer along the bottom of the tank was not evident except within 1 in. of the bottom surface. Excluding a layer of

fluid of 1 in. thickness adjacent to the free surface, upon which free-surface effects might possibly exert an influence, a cylindrical body of fluid 14 in. in diameter and in excess of 3 ft. in height was available free from extraneous disturbances.

The magnitude and distribution of circulation throughout the field of laminar flow of the vortex were measured by timing the motion of a globule of dye judiciously inserted into the water so as to impart an initial momentum equal to that of the ambient fluid.

The path of the globule, in general being helical, appeared as a concentric circle when viewed parallel to the axis of the tank (see figure 8). The radius of such a path was measured and the angular velocity of the globule was clocked over a complete circle, or over a marked arc. Care was taken to obviate errors in measurement ensuing from parallax effects. Also, precautions were taken to preclude possible errors due to precessional motion of the vortex filament by eliminating measurements for which such precession occurred. Measurements were taken only after steady conditions were established. Approximately 45 min were required for the flow to reach a new steady state after altering the value of the circulation.

The circulation was calculated from the formula

$$\Gamma = 2\pi r^2 \omega, \tag{91}$$

where ω is the angular velocity of the globule and r the radius of its path. It was found that, with the exception of an inner cylinder of radius $r \approx 1{\cdot}5$ in., the circulation was constant with radius as well as with depth. The value of the circulation in the potential flow field of the vortex sink is indicated by Γ_∞. The circulation Γ_∞ was varied from one experiment to the next by varying the rate of flow through the vortex tank, to which it was proportional. Any value of circulation could be established in the range between $\Gamma_{\infty_{\min}} = 5{\cdot}5\,\text{in.}^2/\text{sec}$ and $\Gamma_{\infty_{\max}} = 17\,\text{in.}^2/\text{sec}$. At a circulation lower than $\Gamma_{\infty_{\min}}$, precessional oscillations of large period made systematic measurements difficult; at a circulation larger than $\Gamma_{\infty_{\max}}$, entry of air altered the flow in the region of the core, thereby precluding its investigation.

7.3. *Measurement of vorticity along the centre line of the vortex*

A special technique was developed to measure the vorticity along the centre line. It allowed signals of a beam of light reflected from a surface rotating with the fluid to be recorded. The reflecting surface was incorporated in a tracer device of neutral buoyancy which, while being carried with the sink flow along the axis of the vortex, rotated at very nearly the local angular velocity of the fluid. Close agreement between the angular velocity of the tracers and that of the fluid was favoured by their very low moment of inertia about their axis of rotation and by the fact that the radial variation of the axial component of vorticity at the axis of the vortex is zero since the vorticity has its maximum there.

The indicator shown in figure 6 had the appearance of a low-wing airplane in tail-spin attitude. It consisted of a rectangular piece of thin reflecting aluminium foil of $\frac{1}{4}$ in. to $\frac{1}{2}$ in. span and $\frac{1}{8}$ in. chord to which a cylindrical body of buoyant material was glued at mid-span, projecting toward one side of the wing so as to

place the centre of buoyancy above the centre of gravity. Neutral buoyancy and proper spinning characteristics were obtained by trimming this object with a pair of scissors.

Photographic records of the travel of these sensor devices were obtained by training a light beam along the vortex axis in the otherwise darkened area. Upon launching a sensor, a line of dots of light was obtained on the film of a camera with open shutter trained upon the vortex axis. The distance between dots indicated axial displacement and, since the axial velocity was known from other measurements, it provided a time scale. Each dot marked a half revolution of the sensor.

7.4. *Variation of centre-line vorticity with circulation*

Measurements of the vorticity on the centre line of the vortex were obtained by the rotation-tracer technique at three axial locations, for several values of free-stream circulation Γ_∞. The results, figure 7, show that γ_0 varies as the square of the circulation

$$\gamma_0 \propto \Gamma_\infty^2. \tag{92}$$

This result confirms an earlier result, that the core radius r_c varies inversely as the square root of the circulation,

$$r_c \propto 1/\sqrt{\Gamma_\infty}, \tag{93}$$

since equation (A 2)

$$\gamma_0 \pi r_c^2 = k\Gamma_\infty = \text{const.}, \tag{94}$$

or

$$\gamma_0 \eta_c = k\{\Gamma_\infty/(\pi r_0^2)\} \tag{95}$$

for similar $\gamma(r)$ profiles.

The centre-line vorticity, as seen from figure 7, was found to increase toward the vortex sink, corresponding with the decrease of core radius.

7.5. *Radial distribution of vorticity*

The radial distribution of vorticity was measured as a function of radius at various axial locations. Typical results plotted in the form $\gamma(r)/\gamma_0$ vs. r, for a given value of circulation $\Gamma_\infty = 9{\cdot}42\,\text{in.}^2/\text{sec}$ at the axial station $\xi = 0{\cdot}34$ are shown in figure 9. The experimental point on the axis of rotation was obtained by the airfoil-indicator technique described in § 7.3.

Points in the viscous core and in the potential field were obtained by time-exposure photographs of the motion of globules that were injected into the flow at predetermined axial and radial stations. A typical result is shown in figure 8. The globules consisted of a mixture of bromo-naphthalene, paraffin oil and Sudan III dye.

The curvature of the slope near the vortex core was obtained by equating the area under the curve to the circulation. The core radius was obtained from the intersection of a parabola, osculating about the centre line, with the abscissa.

7.6. *Axial velocity along centre line*

Axial velocity distributions along the centre line were measured by timing the motion of dye globules. It can be stated with sufficient accuracy for present purposes that axial flow occurs only in the core for this experiment. The axial

velocity w_0 was determined by placing a drop of dye of near neutral buoyancy on the free surface of the water at the centre of rotation. This dye formed a thread with a clearly discernible front, the progress of which was timed throughout the length of the vortex filament. Local velocities were calculated from measured average values for various values of free-stream circulation Γ_∞, and reduced ratios w_0/Γ_∞^2 were plotted in figure 7. This resulted in a single curve, from which individual points of measurement deviated very little. Characteristics of the curve close to the free surface cannot be discussed, since insufficient measurements are available for this region.

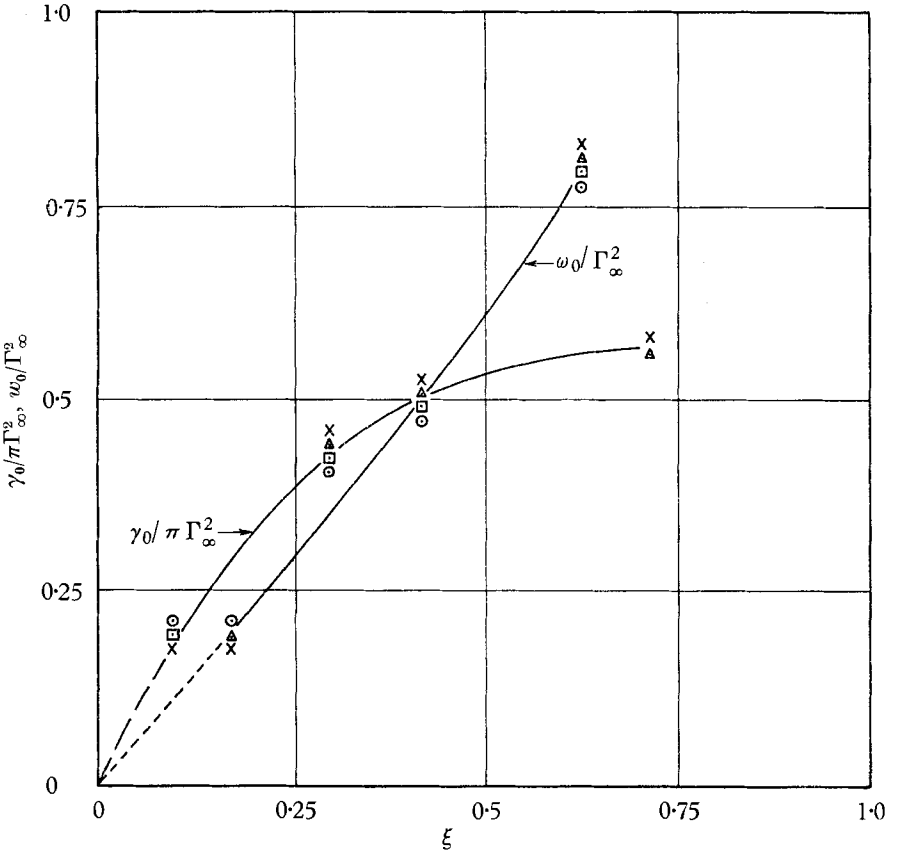

FIGURE 7. Variation of vorticity and axial velocity along the vortex axis.
⊙, Γ_∞ = 5·35 in.²/sec; ⊡, Γ_∞ = 8·15 in.²/sec; △, Γ_∞ = 8·8 in./sec; ×, Γ_∞ = 12·6 in./sec.

7.7. *Radial variation of axial velocity*

The hydrogen-bubble technique was found useful in measuring the radial distribution of the axial velocity in the region where the dye technique failed. A silver wire of approximately 0·003 in. diameter was stretched horizontally diametrically across the vortex core at various depths below the free surface. The elastic supporting wires were bent helically to minimize disturbances. A current pulse was discharged, and within a measured fraction of a second the screen of bubbles produced was illuminated by a light flash and photographed. It was found that

errors in evaluating the radial locations, owing to the peripheral displacement, were negligible. The measured profile of axial velocities was approximated by a Gaussian distribution. A comparison shown in figure 10 reveals significant

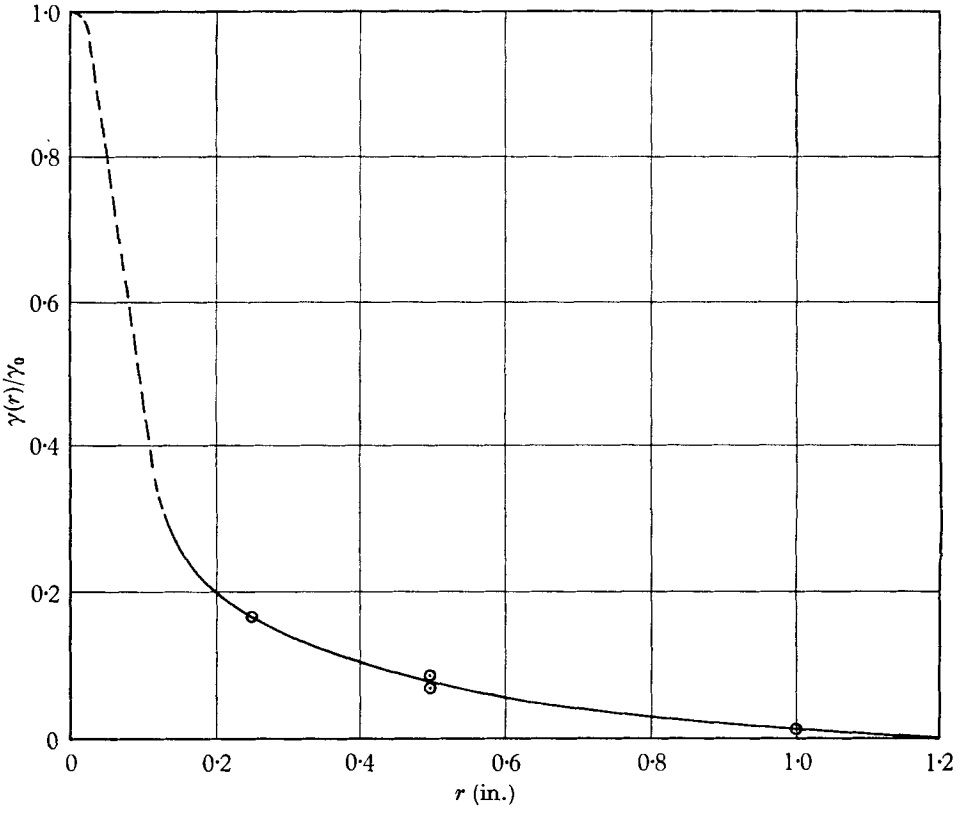

FIGURE 9. Radial variation of vorticity at $\xi = 0{\cdot}34$ for $\Gamma_\infty = 9{\cdot}42$ in.^{2}/sec.

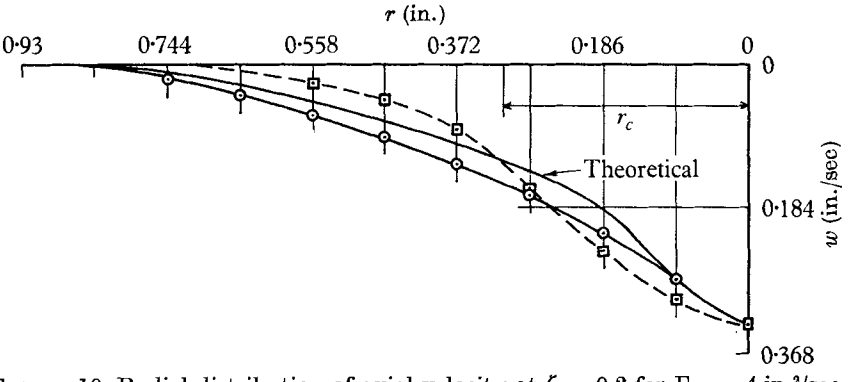

FIGURE 10. Radial distribution of axial velocity at $\xi = 0{\cdot}2$ for $\Gamma_\infty = 4$ in.^{2}/sec.
⊙, Experimental (by hydrogen-bubble technique); ⊡, Gaussian fit.

deviations. Figure 10 does reveal that the core radius obtained by fitting a Gaussian distribution agrees very well with that core radius obtained by vorticity experiments (see figure 11). Furthermore, the theoretical zeroth-order approximation appears inadequate in the core region, as shown in figure 10.

7.8. *Viscous-core radius*

Since the flow was laminar throughout the core, it is natural to surmise that, in the absence of an exact theoretical solution for the steady laminar vortex sink, the core radius varies inversely as the square root of the Reynolds number, as is

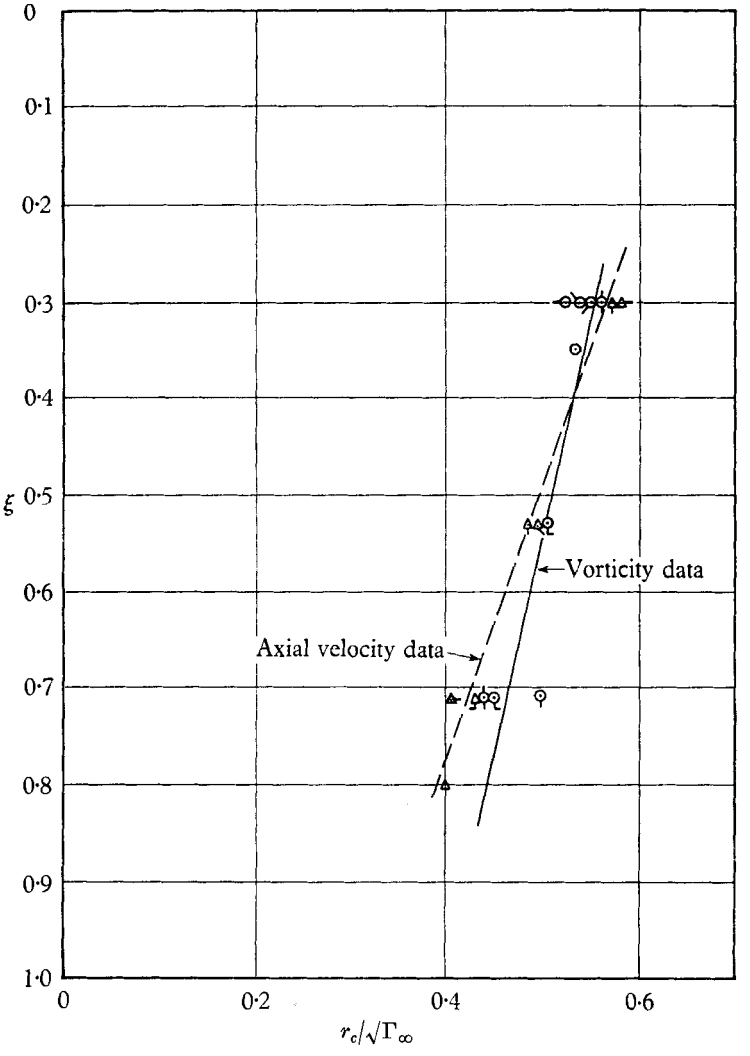

FIGURE 11. Axial variation of core radius. △, ⊙, Averaged results for all axial velocity and vorticity respectively. △, Γ_∞ = 6·04 in.²/sec; ⊙, Γ_∞ = 6·85 in.²/sec; △, Γ_∞ = 7·0 in.²/sec; △, Γ_∞ = 7·9 in.²/sec; △, Γ_∞ = 8·55 in.²/sec; ⊙, Γ_∞ = 9·75 in.²/sec; ⊙, Γ_∞ = 11·2 in.²/sec; ⊙, Γ_∞ = 11·5 in.²/sec; ⊙, Γ_∞ = 12·2 in.²/sec.

the case for laminar boundary layers along solid surfaces. For this reason, the quantity $r_c/\sqrt{\Gamma_\infty}$ was chosen as abscissa in figure 11 since Γ_∞/ν denotes the Reynolds number for the vortex sink.

As seen from figure 11, experimental points of ξ vs. r_c/Γ_∞ confirm the validity of the pre-supposed Reynolds-number function. For obvious reasons, the core

radius on the free surface and on the bottom surface could not be measured. It is seen further from figure 11 that the core radius decreases as the sink is approached and that this decrease appears to be of a logarithmic nature. Also, the diameter of the core based upon radial distribution of axial velocity does not have the same value as that derived from radial-vorticity distribution.

This investigation was sponsored by the Office of Naval Research, United States Department of the Navy, under Contract Number NR 062-376.

Appendix 1. On the core radius

The core radius is the value of the radius for which the forced vortex field meets the free vortex field, or stated alternatively, where the tangential velocity of the potential field is a maximum. The value of the core radius where the tangential velocity is a maximum is, from the equation (7),

$$r_c = \bar{\Gamma}_0(z, r_c)/\partial\bar{\Gamma}_0(z, r_c)/\partial r, \tag{A 1}$$

where $\bar{\Gamma}_0$ is given by equation (32). For instance, vortex motions that are of the Oseen form given by equation (54) (which have been treated by Newman 1959) yields, from equation (A 1),

$$r_c = 1{\cdot}12/\sqrt{f(z)}, \tag{A 2}$$

which states that the core radius is inversely proportional to the square root of the vorticity along the centre line and proportional to the core radius of a Rankine vortex by a factor of 1·12. This justifies the judicious choice of an equivalent Rankine vortex rather than the Oseen vortex for many flow situations.

REFERENCES

BURGERS, J. H. 1956 University of Maryland. *Tech. Note* no. BN-80.

DONALDSON, C. du P. & SULLIVAN, R. D. 1960 *Proc. Heat Transfer & Fluid Mech. Inst.* p. 16.

LEWELLEN, W. S. 1962 *J. Fluid Mech.* **14**, 420.

LONG, R. 1961 *J. Fluid Mech.* **11**, 611.

NEWMAN, B. G. 1959 *Aero Quart.* **10**, 149.

ROTT, N. 1958 *J. Appl. Math. Phys. (ZAMP)*, **9**, 543.

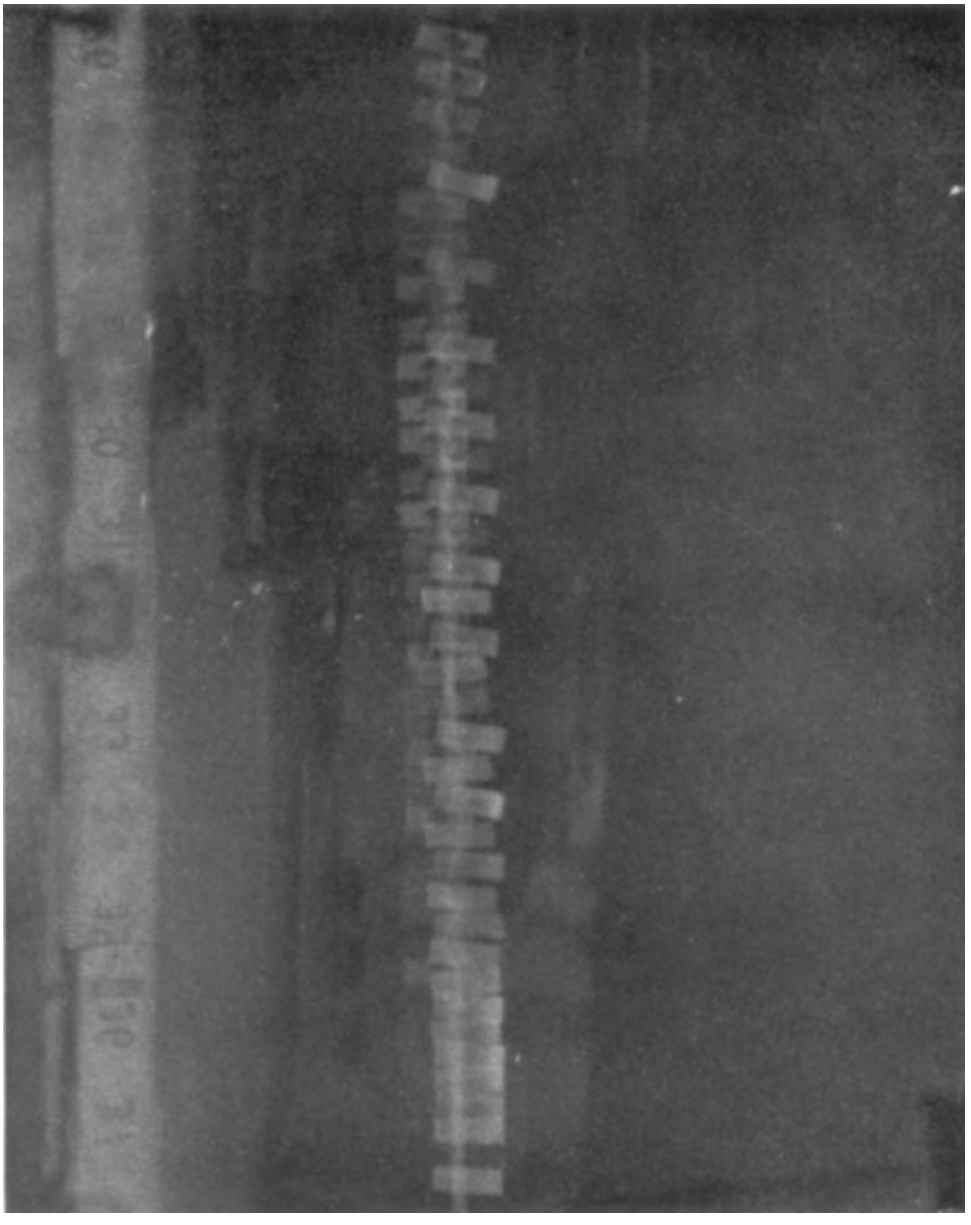

FIGURE 6. Photographic record of indicator motion along axis of rotation.

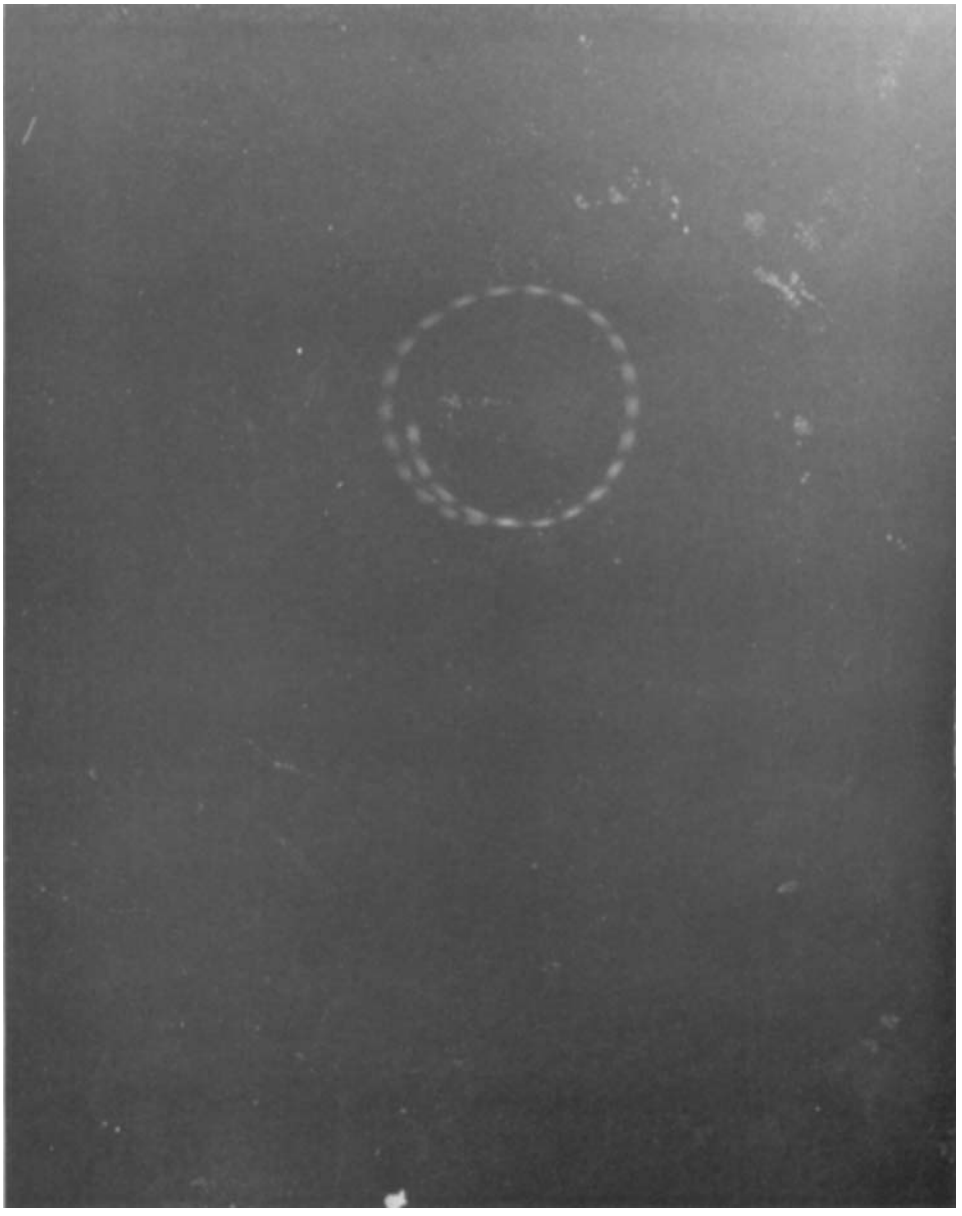

FIGURE 8. Rotational motion (top view) of globule:
radius = 0·275 in., time = 0·5 sec, $\xi = 0{\cdot}34$, $\gamma = 13{\cdot}5$ rad./sec, $\Gamma_\infty = 7{\cdot}9$ in.^{2}/sec.

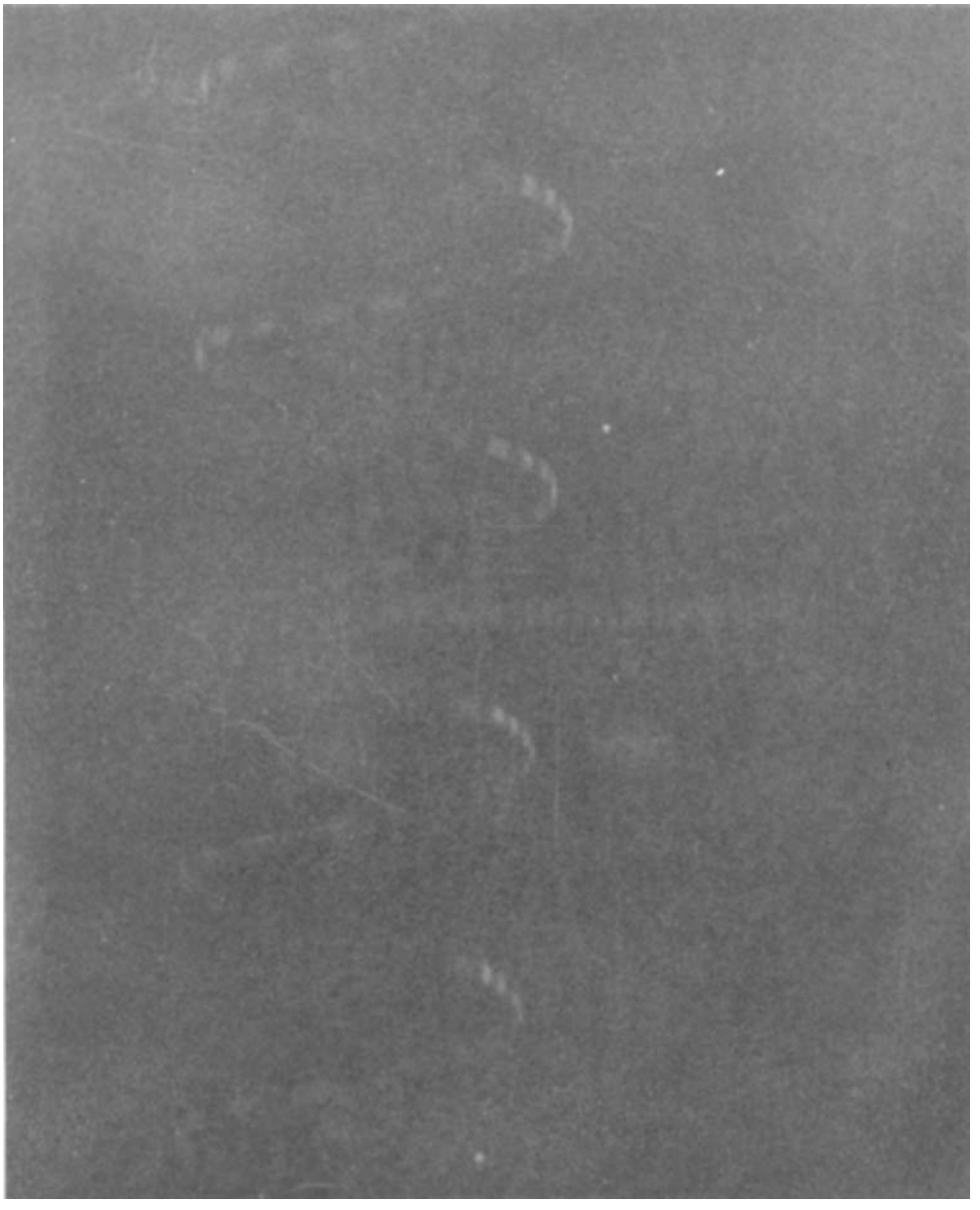

FIGURE 8. Rotational motion (side view) of globule:
radius = 0·313 in., time = 1 sec, $\xi = 0{\cdot}533$, $\gamma = 7$ rad./sec, $\Gamma_\infty = 8{\cdot}5$ in.^{2}/sec.